DØnote 5474-conf

Measurement of the Flavor Oscillation Frequency of B_s^0 Mesons at DØ

The DØ Collaboration

URL: http://www-d0.fnal.gov

(Dated: August 21, 2007)

We present a measurement of the $B_s^0 - \bar{B}_s^0$ oscillation frequency using a large sample of fully reconstructed hadronic and partially reconstructed hadronic and semileptonic B_s^0 decays corresponding to approximately 2.4 fb^{-1} of integrated luminosity accumulated with the DØ Detector in Run II at the Fermilab Tevatron. The flavor of the final state of the B_s^0 meson is determined using the charge of the particle from the reconstructed decay $B_s^0 \to l^+(\pi^+)D_s^- X$, where l^+ is for the semileptonic modes and π^+ is for the hadronic mode. Opposite- and same-side tagging methods are used for the initial-state flavor determination. We perform an unbinned likelihood fit of the proper decay length and obtain $\Delta m_s = 18.56 \pm 0.87(stat.)$ ps^{-1}.

Preliminary Results for Lepton Photon 2007

I. INTRODUCTION

Measurement of the $B_s^0 - \bar{B}_s^0$ oscillation frequency is an important test of the CKM formalism of the Standard Model. The Tevatron is currently the only place where it is possible to make this measurement, which was recently reported by the CDF experiment [1] to be $\Delta m_s = 17.77 \pm 0.10(stat) \pm 0.07(sys)$.

In this analysis we perform a measurement of the $B_s^0 - \bar{B}_s^0$ oscillation frequency that supersedes the previously reported two-sided limit that was published by DØ [2]. In addition to the increase in the statistics of the sample, the following improvements to the analysis were implemented: same-side initial state flavor-tagging, improved decay length resolution due to an additional silicon layer at a very small radius, improved correction for missing particles (the "K-factor"), better modeling of the trigger effects and an event-by-event correction (the " scale factor") to the uncertainty on the visible proper decay length. We also report our first measurement using a hadronic mode.

II. DETECTOR DESCRIPTION

The DØ detector is described in detail elsewhere [3]. The following main elements of the DØ detector are essential for this analysis:

- The magnetic central-tracking system, which consists of a silicon microstrip tracker (SMT) and a central fiber tracker (CFT), both located within a 2-T superconducting solenoidal magnet;
- The muon system located beyond the calorimeter.

The SMT has $\approx 800,000$ individual strips, with typical pitch of $50-80$ μm, and a design optimized for tracking and vertexing capability at $|\eta| < 3$, where $\eta = -\ln(\tan(\theta/2))$ and θ is the polar angle. In addition, the DØ collaboration has installed a new innermost layer of silicon (Layer 0) inside the existing detector during the spring 2006 Tevatron shutdown, which significantly improves the impact parameter resolution for low momentum tracks. The CFT has eight thin coaxial barrels, each supporting two doublets of overlapping scintillating fibers of 0.835-mm diameter, one doublet being parallel to the collision axis, and the other alternating by $\pm 3^\circ$ relative to the axis.

The muon system consists of a layer of tracking detectors and scintillation trigger counters inside a 1.8-T iron toroid, followed by two additional layers outside the toroid. Tracking at $|\eta| < 1$ relies on 10-cm-wide drift tubes, while 1-cm mini-drift tubes are used at $1 < |\eta| < 2$.

The SMT, CFT, and muon systems are described in more detail in reference [4].

III. DATA SAMPLE AND EVENT SELECTION

This analysis was performed with a large inclusive muon sample corresponding to approximately 2.4 fb^{-1} of integrated luminosity selected with an offline filter from all data accumulated by the DØ Detector between April 2002 and May 2007. RunIIa is defined as the time period April 2002 to March 2006 ($1.3 fb^{-1}$ of data) and RunIIb includes all data taken after March 2006 ($1.1 fb^{-1}$ of data). The data were collected by inclusive single muon and di-muon triggers.

For the offline selection, the muons are required to have $p_T > 2$ GeV/c and $p > 3$ GeV/c, to have hits both in the CFT and SMT and to have at least two measurements in the muon chambers. Four B_s^0 meson final states are considered in this analysis (Charge conjugated states are implied throughout the note):

$$B_s^0 \to \pi^+ D_s^- X,\ D_s^- \to \phi\pi^-,\ \phi \to K^+K^-, \tag{1}$$
$$B_s^0 \to \mu^+ D_s^- X,\ D_s^- \to \phi\pi^-,\ \phi \to K^+K^-, \tag{2}$$
$$B_s^0 \to e^+ D_s^- X,\ D_s^- \to \phi\pi^-,\ \phi \to K^+K^-, \tag{3}$$
$$B_s^0 \to \mu^+ D_s^- X,\ D_s^- \to K^{*0}K^-,\ K^{*0} \to K^+\pi^- \tag{4}$$

All charged particles in the event were clustered into jets using the DURHAM clustering algorithm [6] with a p_T cut-off parameter set at 15 GeV/c [7].

The reconstruction of the $B_s^0 \to l^+ D_s^-$ decay starts by forming the D_s^- candidates. The D_s^- candidate is constructed from three tracks included in the same jet. For the $D_s^- \to \phi\pi$ decay mode, two oppositely charged tracks are assigned the kaon mass (K_1 and K_2) and are required to form a ϕ meson satisfying $1.004 < M(K^+K^-) < 1.034$ GeV/c^2. The third track must have a charge opposite to the lepton charge, or the pion charge in the case of the hadronic mode. For the $D_s^- \to K^{*0}K$ decay mode, three tracks are selected according to the charge combination $\mu^+ K_1^+ K_2^- \pi^-$ or its

$l^+D_s^-(D_s^- \to \phi\pi^-)$	$\pi^+D_s^-(D_s^- \to \phi\pi^-)$	$\mu^+D_s^-(D_s^- \to K^{*0}K^-)$
$p_{\rm T}(\pi) > 0.5$ Gev/c	$p_{\rm T}(\pi) > 0.5$ Gev/c	$p_{\rm T}(\pi) > 0.5$ Gev/c
$p_{\rm T}(K_1) > 0.7$ Gev/c	$p_{\rm T}(K_1) > 0.5$ Gev/c	$p_{\rm T}(K_1) > 0.9$ Gev/c
$p_{\rm T}(K_2) > 0.7$ Gev/c	$p_{\rm T}(K_2) > 0.5$ Gev/c	$p_{\rm T}(K_2) > 1.8$ Gev/c
$1.004 < m(K_1,K_2) < 1.034$ GeV/c^2	$1.014 < m(K_1,K_2) < 1.026$ GeV/c^2	$0.82 < m(K_1,\pi) < 0.95$ GeV/c^2

TABLE I: Kinematic event selection criteria

charge conjugate. The K_1 and K_2 tracks are assigned the kaon mass and the third track is assigned the pion mass. The K_1 track is assumed to come from the $K^{*0} \to K^+\pi^-$ decay. All three tracks must have hits in the SMT and CFT. For each particle, the transverse, ϵ_T, and longitudinal, ϵ_L, projections of the track impact parameter with respect to the primary vertex, together with the corresponding uncertainties $\sigma(\epsilon_T)$ and $\sigma(\epsilon_L)$, are computed. The combined significance $(\epsilon_T/\sigma(\epsilon_T))^2 + (\epsilon_L/\sigma(\epsilon_L))^2$ is required to exceed four for the kaons. In addition, the impact parameter significance of the pion is required to exceed 8.5 in the $\pi\phi\pi$ decay mode. The selection requirements specific to each decay mode are summarized in Table I.

The three tracks must form a common D_s vertex with $\chi^2_D < 16$ for the vertex fit. The vertexing algorithm is described in detail in [9]. The distance d_T^D between the primary and D_s vertices in the transverse plane is required to exceed four standard deviations, that is, $d_T^D/\sigma(d_T^D) > 4$. The angle α_T^D between the D_s^- momentum and the direction from the primary vertex to the D_s^- vertex in the transverse plane must satisfy the condition $\cos(\alpha_T^D) > 0.9$.

We add a lepton or a track with assigned pion mass to form a B_s^0 candidate. In the hadronic mode, the impact parameter significance of the pion track has to be larger than six and to have a minimum transverse momentum of at least 3.0 GeV/c. The tracks of the lepton or pion and D_s^- candidate are required to produce a common B_s vertex with $\chi^2_B < 9$ for the vertex fit. In the electron and hadronic modes, an offline-selected muon is required to be outside the jet of the D_s^- meson. The charge of this muon is used to tag the flavor of the reconstructed B_s meson. The transverse momentum of the B_s hadron, $p_T^{lD_s^-}$, is defined as the vector sum of the transverse momenta of the muon (electron) and the D_s^- candidate. The mass of the $(l^+D_s^-)$ system must be within the range $2.6 < M(l^+D_s^-) < 5.4$ GeV/c^2. The transverse decay length of the B_s^0 hadron, d_T^B, is defined as the distance in the transverse plane between the primary vertex and the vertex produced by the lepton (pion) and the D_s^- meson. If the distance d_T^B exceeds $4 \cdot \sigma(d_T^B)$, the angle α_T^B between the B_s momentum and the direction from the primary to the B vertex in the transverse plane is required to satisfy the condition $\cos(\alpha_T^B) > 0.95$. The distance d_T^B is allowed to be greater than d_T^D, provided that the distance between the B and D vertices, d_T^{BD}, is less than $2 \cdot \sigma(d_T^{BD})$.

The final event samples were selected using a likelihood ratio method, described below.

Likelihood Ratio Method

In the Likelihood Ratio Method, a set of discriminating variables, $x_1, ...x_n$, is constructed for a given event. The probability density functions, $f^s(x_i)$ for the signal and $f^b(x_i)$ for the background, are built for each variable x_i. The combined tagging variable y is defined as

$$y = \prod_{i=1}^{n} y_i; \quad y_i = \frac{f_i^b(x_i)}{f_i^s(x_i)}. \tag{5}$$

The variable x_i can be undefined for some events. In this case, the corresponding variable y_i is set to unity. The selection of the signal is obtained by applying the cut $y < y_0$. For uncorrelated variables $x_1, ...x_n$, the selection using the combined variable y gives the best possible performance, i.e., the maximal signal efficiency for a given background efficiency.

The following discriminating variables are used:

- Helicity angle, defined as the angle between the D_s and K_1 momenta in the (K_1, K_2) center-of-mass system, or $K_1\pi$ in the case of the $K^{*0}K$;
- Isolation, computed as $Iso = p^{tot}(lD_s)/(p^{tot}(lD_s) + \sum p_i^{tot})$. The sum $\sum p_i^{tot}$ is taken over all charged particles in the cone $\sqrt{(\Delta\phi)^2 + (\Delta\eta)^2} < 0.5$, where $\Delta\eta$ and $\Delta\phi$ are the pseudorapidity and the azimuthal angle with respect to the (lD_s) direction. The lepton, K_1, K_2 and π momenta are not included in the sum;
- $p_T(K_1K_2)$, or $p_T(K_2)$ in the case of the $K^{*0}K$;
- Invariant mass, $M(lD_s)$ (not used in the hadronic mode);

Channel	Run IIa	RunIIb	Total
$\mu^+ D_s^-,\ D_s^- \to \phi\pi^-$	28238 ± 339	16539 ± 239	44777 ± 415
$e^+ D_s^-,\ D_s^- \to \phi\pi^-$	1142 ± 83	548 ± 45	1663 ± 102
$\pi^+ D_s^-,\ D_s^- \to \phi\pi^-$	159 ± 13	90 ± 11	249 ± 17
$\mu^+ D_s^-,\ D_s^- \to K^{*0}K^-$	11649 ± 661	6449 ± 616	18098 ± 903

TABLE II: Number of signal candidates

- χ^2 of the D_s vertex fit;
- Invariant mass, $M(K_1K_2)$, or $M(K_1\pi)$ in the case of the $K^{*0}K$.

The probability density functions are constructed using the real data events. For each channel, three bands, B_1, B_2 and S are defined as:

$$\begin{aligned} B_1 &: 1.75 < M(D_s) < 1.79\ \text{GeV}/c^2; \\ B_2 &: 2.13 < M(D_s) < 2.17\ \text{GeV}/c^2; \\ S &: 1.92 < M(D_s) < 2.00\ \text{GeV}/c^2. \end{aligned}$$

The background probability density function (PDF) for each variable is constructed using events from the B_1 and B_2 bands. The signal probability density function is constructed by subtracting the background, obtained as a sum of the distributions in the B_1 and B_2 bands, from the distribution of events in band S. The final cut on the combined variable, $\log_{10} y < 0.12$, is selected by requiring the maximal value of $S/\sqrt{S+B_1+B_2}$.

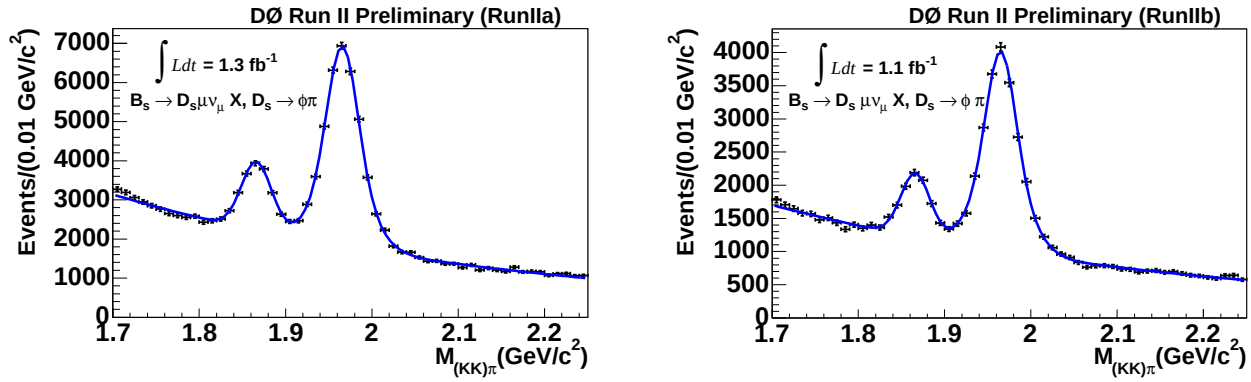

FIG. 1: D_s^+ invariant mass distribution in the $\mu\phi\pi$ decay mode for the RunIIa (left) and RunIIb (right) periods, respectively. The left and right peaks on the plots correspond to the $\mu(e)D^{\pm}$ and $\mu(e)D_s$ candidates, respectively. The curve represents the fit function to the mass spectrum.

The total number of D_s^-candidates passing this combined variable cut in the mass peak is summarized in Table II for each data taking period for all modes. The hadronic and semielectronic decay modes are also selected from the sample triggered by the muon, and hence most of the events in these two decay modes are muon tagged events. The mass distributions of the D_s^-candidates are shown in Figs. 1 - 3.
Since the $\mu K^{*0}K^{\pm}$ channel is dominated by the large reflections coming from the mis-identification of a pion track as a kaon track, extracting the signal in this channel becomes difficult. In order to separate the signal from the reflections, an event-by-event likelihood fit was developed. This technique is based on the kinematic properties of the events and is discussed in detail in Ref. [10].

IV. FLAVOR TAGGING

A necessary step in the B_s^0 oscillation analysis is the determination of the $B_s^0/\bar{B}_s^0$ initial- and final-state flavors. The presence of the lepton (pion) in the B_s^0 semi-leptonic (hadronic) decay allows a determination of the final-state flavor using the relations $B_s^0 \to l^+X$ and $\bar{B}_s^0 \to l^-X$ ($B_s^0 \to \pi^+X$ and $\bar{B}_s^0 \to \pi^-X$).

The flavor of the B_s^0 at production is determined using both opposite- and same-side flavor tagging techniques. Purity, dilution and tagging efficiency are three important parameters for describing the tagging performance. The purity

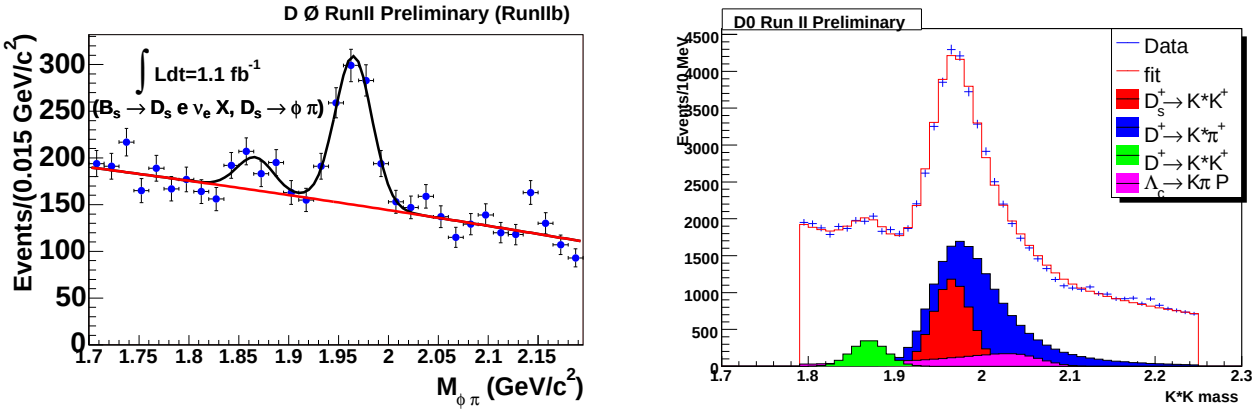

FIG. 2: D_s^+ invariant mass distribution for the RunIIb B_s^0 sample. The left and right plots show the $e\phi\pi$ and $\mu K^{*0}K$ decay channels, respectively. The left and right peaks on the plots correspond to the $\mu D^{\pm}$ and μD_s candidates, respectively. The curve represents the fit function to the mass spectrum.

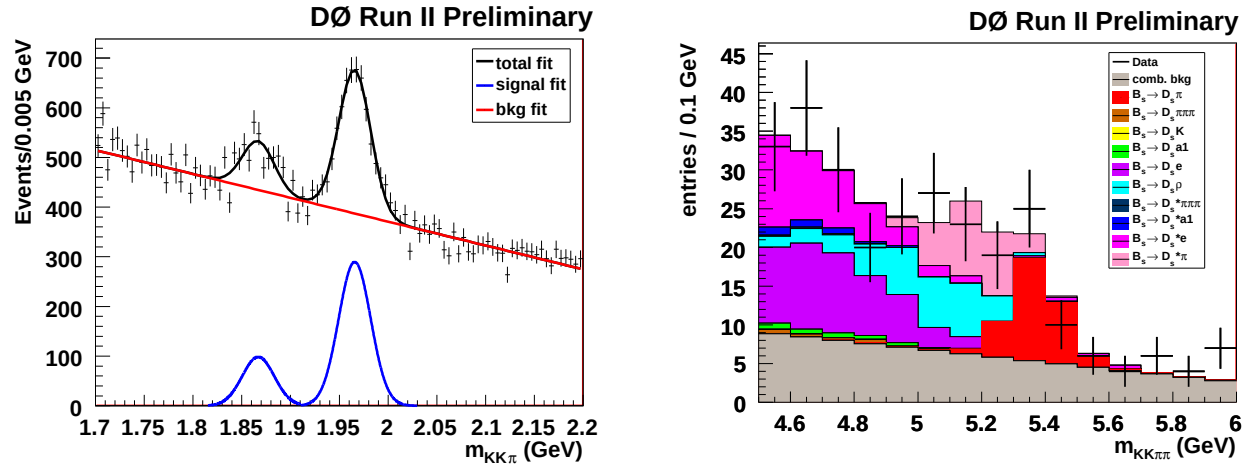

FIG. 3: The plot on the left is the D_s^+ invariant mass distribution for the untagged RunIIa B_s^0 sample in the hadronic mode $D_s(\phi\pi)\pi$. The plot on the right is the B_s^0 invariant mass distribution for the untagged RunIIa data sample in the hadronic decay mode $D_s(\phi\pi)\pi$.

of the tagging method is defined as $\eta_s = N_{correctly\ tagged\ events}/N_{total\ tagged\ events}$. The dilution is related to the purity by the simple formula $\mathcal{D} = 2\eta_s - 1$. Finally, the tagging efficiency is defined as $\epsilon = N_{total\ tagged\ events}/N_{total\ events}$.

A likelihood ratio method was used to combine the different taggers, where a set of flavor discriminating variables $x_1, ..., x_n$ was constructed for each event. Then, a combined tagging variable y is constructed:

$$y = \prod_{i=1}^{n} y_i; \quad y_i = \frac{f_i^{\bar{b}}(x_i)}{f_i^{b}(x_i)}, \tag{6}$$

where the $f_i^b(x_i)$ is the probability density function (PDF) for each discriminating variable described above. It is more convenient to define the tagging variable as

$$d = \frac{1-y}{1+y}. \tag{7}$$

The parameter d varies between -1 and 1. An event with $d > 0$ is tagged as b quark and that with $d < 0$ as a $\bar{b}$ quark, with larger $|d|$ values corresponding to higher tagging purities.

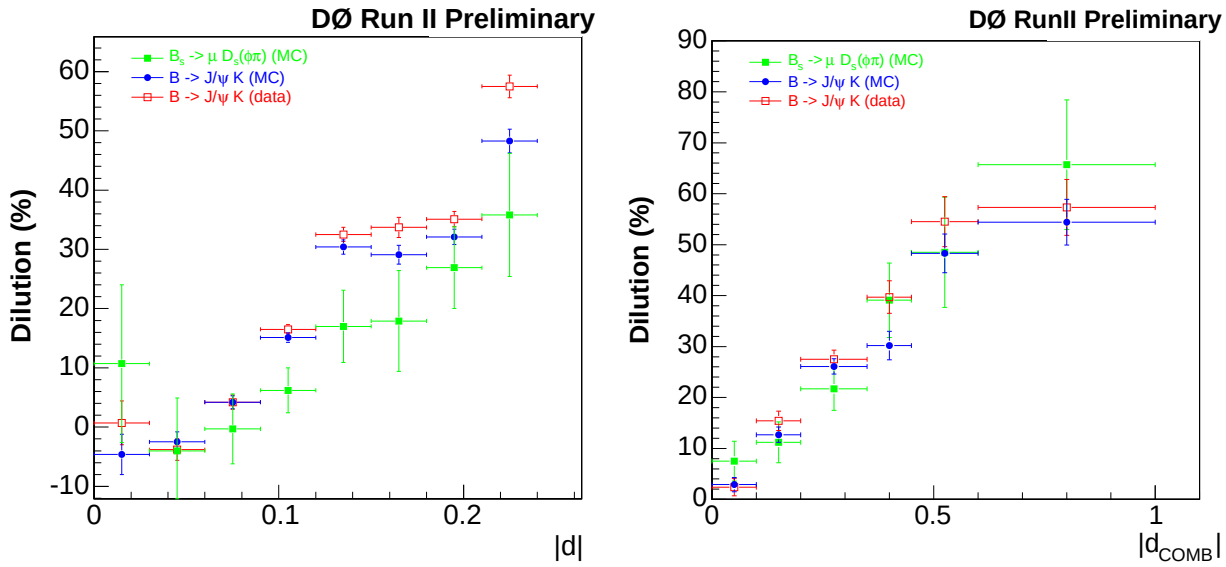

FIG. 4: Dilution versus variable $|d_{SST}|$ for same-side tagger (Left) and the combined tagger (OST+SST) (Right) in the $B^+ \to J/\psi K^+$ sample (MC and data) and for $B_s \to \mu D_s(\phi\pi)$ (MC).

A. Opposite-Side Tagging

The opposite-side tagging (OST) of the initial flavor of the B_s meson, which exploits the presence of a muon or an electron and/or a secondary vertex on the opposite side, is described elsewhere [11]. The dilution for OST is measured in data using large samples of semileptonic decays of B_u mesons, which do not oscillate, and B_d mesons, which do. The OST tagger is used in all the B_s^0 decay modes.

B. Same-Side Tagging

The same-side tagging (SST) technique uses the properties of the particles produced in association with the reconstructed B_s^0 meson. We consider single-track and multiple-track based taggers. For the single-track tagger, we select a track with the minimum distance $\Delta R = \sqrt{\Delta\phi^2 + \Delta\eta^2}$ between the tag track and the momentum of the reconstructed B meson candidate, where $\Delta\eta$ and $\Delta\phi$ are the pseudo-rapidity and the azimuthal angle with respect to the B meson direction. For the multiple-track tagger, we use all the tracks in a cone defined by $\cos\alpha x(p, p_B) > 0.8$ around the B meson's momentum. We combine these two taggers according to the algorithm developed for OST [11] and introduce a *combined variable* d_{SST}. We predict the dilution of the combined SST by taking a weighted average of dilutions from the two Monte Carlo (MC) samples of $B_s^0\mu^+D_s^-$, $D_s^- \to \phi\pi^-$ and $B_s^0 \to J/\psi\phi$ decays. To verify the prediction of the simulation, we measure the dilution in a control sample of $B^+ \to J/\psi K^+$ decays both in the data and MC. This is possible since B^+ mesons do not oscillate and we can infer their flavor from the sign of the charged kaon and compare it to the flavor determined by the tagger. The comparison of data and MC for SST is shown in Fig. 4 (Left).

C. The Combined Tag

In the $\mu\phi\pi$ mode, a combined OST-SST tagger is used. The combination is done as follows. For the events where OST is not defined, we add an opposite-side flavor tagger, "event-charge", based on all the tracks outside of the cone $\cos\alpha > 0.8$ around the B_s momentum direction. If both an OST and an SST tag are present, we combine them assuming they are independent. Otherwise, we combine information from the "event-charge" tagger with SST.

The dependence of the dilution of the OST-STT combination on the magnitude of the variable $|d_{COMB}|$ is shown

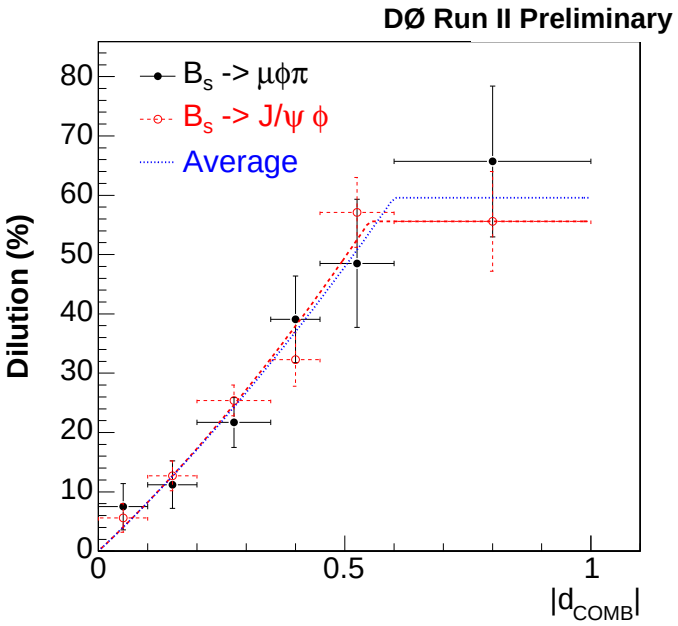

FIG. 5: Dilution versus variable $|d_{COMB}|$ for combined same-side and opposite-side taggers for $B_s \to J/\psi\phi$ events and for $B_s \to \mu D_s(\phi\pi)$ (MC) with parametrization function superimposed.

in Fig. 4(Right) and in Fig. 5. We parametrize it with the following function:

$$\begin{aligned} \mathcal{D}(d_{COMB}) &= 0.7895|d_{COMB}| + 0.3390|d_{COMB}|^2, \ |d_{COMB}| < 0.6 \\ \mathcal{D}(d_{COMB}) &= 0.6065|d_{COMB}|, \ |d_{COMB}| > 0.6 \end{aligned} \tag{8}$$

The total combined tagging power is $\epsilon D^2 = (4.49 \pm 0.88)\%$. This is larger than the individual tagging powers of SST and OST. A more detailed description of SST and its combination with OST is given in Reference [12].

V. EXPERIMENTAL OBSERVABLES

Semi-leptonic B decays necessarily have an undetected neutrino present in the decay chain, making a precise determination of the kinematics for the B meson impossible. In addition, in partially reconstructed hadronic- and semileptonic decays, other neutral or non-reconstructed charged particles can be present in the decay chain of the B meson. This leads to a bias towards smaller values of the B momentum, which is calculated using the reconstructed particles. A common practice to correct this bias is to scale the measured momentum of the B candidate by a K factor, which takes into account the effects of neutrinos and other lost or non-reconstructed particles. The K factor is estimated from the MC simulation. For this analysis, it was defined as

$$K = p_T(l(\pi)D_s)/p_T(B), \tag{9}$$

where p_T denotes the absolute value of the transverse momentum. The K factor equals 1 in the fully reconstructed hadronic decays.

The proper lifetime of the B_s^0 meson, $ct_{B_s^0}$, can be written as

$$ct_{B_s^0} = x^M \cdot K, \quad \text{where} \quad x^M = (\mathbf{d_T^B} \cdot \mathbf{p_{xy}^{\mu D_s^-}})/(p_T^{\mu D_s^-})^2 \cdot M_B. \tag{10}$$

x^M is the *visible proper decay length* or VPDL.

VI. FITTING PROCEDURE

For the extraction of the oscillation frequency Δm_s, a maximum likelihood method has been used.

A. Semileptonic Decay Modes

All tagged events with $1.72 < M((K^+K^-)\pi) < 2.22$ GeV/c^2 were used in the unbinned likelihood fitting procedure. The likelihood for an event to arise from a specific source in the sample depends on x^M, its uncertainty (σ_{x^M}), the mass of the D_s^- meson candidate (m) and the predicted dilution (d_{pr}). In addition, we include the $\log_{10} y$ selection variable described in Section III. All of these quantities are known on an event-by-event basis. The PDF for each source can be expressed by the product of the corresponding PDFs:

$$f_i = P_i^{x^M}(x^M, \sigma_{x^M}, d_{pr}) P_i^{\sigma_{x^M}} P_i^m P_i^{d_{pr}} P_i^{log_{10} y}. \tag{11}$$

The following sources were considered:

- lD_s signal with fraction $\mathcal{F}_{lD_s}$.
- $lD^\pm$ signal with fraction $\mathcal{F}_{lD^\pm}$.
- $lD^\pm(\rightarrow K\pi\pi)$ reflection with fraction $\mathcal{F}_{lD^\pm_{refl}}$. The reflection arises due to mass misassignment in this decay channel. The $D^\pm$ mass peak shifts to ~ 2 GeV/c^2 if the kaon mass is assigned to one of the pion tracks. A $\mu\Lambda^\pm(\rightarrow K\pi P)$ reflection with fraction $\mathcal{F}_{\mu\Lambda^\pm_{refl}}$ is also added for $\mu K^{*0} K$ channel.
- Combinatorial background with fraction $(1 - \mathcal{F}_{lD_s} - \mathcal{F}_{lD^\pm} - \mathcal{F}_{lD^\pm_{refl}})$.

The fractions $\mathcal{F}_{lD_s}$ and $\mathcal{F}_{lD^\pm}$ are determined from the mass fit. The total probability density function for a B candidate has the form

$$F_n = \mathcal{F}_{lD_s} f_{lD_s} + \mathcal{F}_{lD^\pm} f_{lD^\pm} + \mathcal{F}_{lD^\pm_{refl}} f_{lD^\pm_{refl}} + \left(1 - \mathcal{F}_{lD_s} - \mathcal{F}_{lD^\pm} - \mathcal{F}_{lD^\pm_{refl}}\right) f_{bkg}. \tag{12}$$

The following form was minimized using the MINUIT [13] program:

$$\mathcal{L} = -2 \sum_{n=1}^{N_{candidates}} \ln F_n \tag{13}$$

The PDFs for the VPDL uncertainty ($P_i^{\sigma_{x^M}}$), mass (P_i^m) and dilution ($P_i^{d_{pr}}$) are taken from experimental data. The signal PDFs are also used for the $lD^\pm$ signal and the reflections. The mass PDF for the $lD^\pm(\rightarrow K\pi\pi)$ reflection is determined from the MC simulation. The fractions of $K\pi\pi$ and $K\pi P$ reflected events under the D_s^- mass peak are determined using a fit to the full untagged mass spectrum (Fig. 2 (right)).

B. Hadronic Decay Mode

For calculating the PDFs, we start with a VPDL template for every fixed Δm_s value including the B_s^0 decay time distribution folded with the oscillation. The templates are then folded with the efficiency curve for short VPDL, with the individual resolution function of each event and with a K factor, depending on the visible B_s^0 mass, to correct for non-reconstructed particles. The result is a Δm_s-dependent probability density template P_{osc} for every individual event. The same procedure is done for a template including the non-oscillated hypothesis P_{n-osc} (oscillation with $1 - \cos\ \Delta m_s$ instead of $1 + \cos\ \Delta m_s$). The dilution $\mathcal{D}$ is corrected for the expected background fraction (which has dilution 0). Afterwards, the event-wise oscillation probability P_{evt} is calculated with the following formula:

$$P_{evt} = (xP_{osc} - (1-x)P_{n-osc})/(P_{osc} + P_{n-osc}), \tag{14}$$

where $x = (1 + \mathcal{D})/2$, $\mathcal{D}$ is the background corrected dilution for the event and $P_{osc} + P_{n-osc}$ is the normalization factor.

C. PDF for lD_s Signal

The lD_s sample is composed mostly of B_s^0 mesons with some contributions from B_u and B_d mesons. Different species of B mesons behave differently with respect to oscillations. Neutral B_d and B_s mesons do oscillate (with

different frequencies) while charged B_u mesons do not. The possible contributions of b baryons to the sample are expected to be small and so are neglected.

The data sample is divided into non-oscillated and oscillated subsamples as determined by the flavor tagging. For a given type of B hadron (i.e., d, u, s), the distribution of the visible proper decay length x for non-oscillated and oscillated cases (p^{nos} and p^{osc}) is given by:

$$p_s^{nos}(x,K,d_{pr}) = \frac{K}{c\tau_{B_s}} \exp(-\frac{Kx}{c\tau_{B_s}}) \cdot 0.5 \cdot (1 + \mathcal{D}(d_{pr}) \cos(\Delta m_s \cdot Kx/c)) \tag{15}$$

$$p_s^{osc}(x,K,d_{pr}) = \frac{K}{c\tau_{B_s}} \exp(-\frac{Kx}{c\tau_{B_s}}) \cdot 0.5 \cdot (1 - \mathcal{D}(d_{pr}) \cos(\Delta m_s \cdot Kx/c)) \tag{16}$$

$$p_{DsDs}^{osc}(x,K) = \frac{K}{c\tau_{B_s}} \exp(-\frac{Kx}{c\tau_{B_s}}) \cdot 0.5 \tag{17}$$

$$p_{DsDs}^{nos}(x,K) = \frac{K}{c\tau_{B_s}} \exp(-\frac{Kx}{c\tau_{B_s}}) \cdot 0.5 \tag{18}$$

$$p_u^{nos}(x,K,d_{pr}) = \frac{K}{c\tau_{B_u}} \exp(-\frac{Kx}{c\tau_{B_u}}) \cdot 0.5 \cdot (1 - \mathcal{D}(d_{pr})) \tag{19}$$

$$p_u^{osc}(x,K,d_{pr}) = \frac{K}{c\tau_{B_u}} \exp(-\frac{Kx}{c\tau_{B_u}}) \cdot 0.5 \cdot (1 + \mathcal{D}(d_{pr})) \tag{20}$$

$$p_d^{nos}(x,K,d_{pr}) = \frac{K}{c\tau_{B_d}} \exp(-\frac{Kx}{c\tau_{B_d}}) \cdot 0.5 \cdot (1 - \mathcal{D}(d_{pr}) \cos(\Delta m_d \cdot Kx/c)) \tag{21}$$

$$p_d^{osc}(x,K,d_{pr}) = \frac{K}{c\tau_{B_d}} \exp(-\frac{Kx}{c\tau_{B_d}}) \cdot 0.5 \cdot (1 + \mathcal{D}(d_{pr}) \cos(\Delta m_d \cdot Kx/c)). \tag{22}$$

Here τ_{B_q} is the lifetime of the B_q hadron, where q is u, d, or s. Note that there is a sign swap in Eqns. 19–22 with respect to Eqns. 15 and 16 due to anti-correlation of charge for muons from $B \to DD_s$; $D \to lX$ processes.

The translation to the measured VPDL, x^M, is achieved by a convolution of the K factors and resolution functions as specified below.

$$P_j^{osc,\ nos}(x^M, \sigma_{x^M}, d_{pr}) \ = \tag{23}$$
$$\int_{K_{min}}^{K_{max}} dK\ D_j(K) \cdot \frac{Eff_j(x^M)}{N_j(K, \sigma_{x^M}, d_{pr})} \qquad \int_0^\infty dx\ G(x - x^M, \sigma_{x^M}) \cdot p_j^{osc,\ nos}(x, K, d_{pr}).$$

Here

$$G(x - x^M, \sigma_{x^M}) = \frac{1}{\sqrt{2\pi} s_{sig} \sigma_{x^M}} \exp\left(-\frac{(x - x^M)^2}{2 s_{sig} \sigma_{x^M}^2}\right) \tag{24}$$

is the detector resolution of the VPDL with an additional scale factor s_{sig} (described in VII) and $Eff_j(x)$ is the reconstruction efficiency for a given decay channel j of this type of B meson as a function of VPDL. The function $D_j(K)$ gives the normalized distribution of the K factor in a given channel j. The normalization factor N_j is calculated by integration over the entire VPDL region:

$$N_j(K, \sigma_{x^M}, d_{pr}) \ = \ \int_{-\infty}^{\infty} dx^M\ Eff_j(x^M) \cdot \tag{25}$$
$$\int_0^\infty dx\ G(x - x^M, \sigma_{x^M}) \ \cdot \ \left(p_j^{osc}(x, K, d_{pr}) + p_j^{nos}(x, K, d_{pr})\right)$$

The total VPDL PDF for the lD_s signal is a sum of all the contributions that yield the D_s mass peak:

$$P^{osc,\ nos}_{\mu D_s}(x^M, \sigma_{x^M}, d_{pr}) = (1 - \mathcal{F}_{peak}) \sum_j Br_j \cdot P^{osc,\ nos}_j(x^M, \sigma_{x^M}, d_{pr}) + \mathcal{F}_{peak} \cdot P^{osc,\ nos}_{peak}(x^M) \quad (26)$$

Here the sum $\sum_j$ is taken over all decay channels $B_s \to l^+ \nu D_s^- X$ and Br_j is the branching fraction of a given channel j. In addition to the long-lived B_s candidates, there is a contribution of the "peaking background", which consists of combinations of D_s mesons and muons originating from different c or b quarks. The direct c production gives the largest contribution to this background and, therefore, the function $P^{osc,\ nos}_{peak}(x^M)$ is determined from $c\bar{c}$ MC. We assume that this background does not depend on the tagging.

The branching fractions Br_j were taken from the PDG [8]. The functions $D_j(K)$ and $Eff_j(x)$ were taken from the MC simulation, as explained later. The lifetimes of the B_u and B_d mesons were taken from PDG while the B_s lifetime was measured using the total tagged lD_s sample.

Following the procedure that was used in Ref. [2], we choose to use a technique called the amplitude fit method [15]. This technique requires a modification of Eqs. (15) and (16), yielding the form

$$p^{nos/osc}_s(x, K, d_{pr}) = \frac{K}{c\tau_{B_s}} \exp(-\frac{Kx}{c\tau_{B_s}}) \cdot 0.5 \cdot (1 \pm \mathcal{D}(d_{pr}) \cos(\Delta m_s \cdot Kx/c) \cdot \mathcal{A}), \quad (27)$$

where $\mathcal{A}$ is now the only fit parameter.

The values of Δm_s were changed from 0 ps^{-1} to 30 ps^{-1} with a step size of 0.5 ps^{-1}. By plotting the fitted value of $\mathcal{A}$ as a function of the input value of Δm_s, one searches for a peak of $\mathcal{A}$=1 to obtain a measurement of Δm_s. For any value of Δm_s not equal to the "true" value of the B_s oscillation frequency, the amplitude $\mathcal{A}$ should be zero. If no peak is found, limits can be set on Δm_s using this method. The sensitivity of a measurement is determined by calculating the probability that at a non-"true"value of Δm_s the amplitude could fluctuate to $\mathcal{A}$=1. This occurs at the lowest value of Δm_s for which 1.645 $\sigma_{\Delta m_s} = 1$ for a 95% CL, where $\sigma_{\Delta m_s}$ is the uncertainty on the value of $\mathcal{A}$ at the point Δm_s.

D. PDF for lD_s Combinatorial Background

The following contributions to the combinatorial background were considered:

1. Prompt background with the lD_s vertex coinciding with the primary vertex (described as a Gaussian with a width determined by the resolution; fraction in the background: $\mathcal{F}_0$). The resolution scale factor for this background is different from the signal resolution scale factor. The scale factor is a free fit parameter, s_{bkg}.

2. Background with quasi-vertices distributed around the primary vertex (described as a Gaussian with constant width σ_{peak_bkg}; fraction in the background: $\mathcal{F}_{peak\_bkg}$).

3. Long-lived background (exponential with constant decay length $c\tau_{bkg}$ convoluted with the resolution). This background was divided into three subsamples:

   (a) insensitive to the tagging (fraction in the long-lived background: $(1 - \mathcal{F}_{tsens})$);

   (b) sensitive to the tagging and non-oscillating (fraction in the background sensitive to the tagging: $(1-\mathcal{F}_{osc})$);

   (c) sensitive to the tagging and oscillating with frequency Δm_d (fraction in the background sensitive to the tagging: $\mathcal{F}_{osc}$).

In addition, in the $\mu K^{*0} K$ mode negative $c\tau_{NegExp}$ and positive $c\tau_{long}$ exponential components with fractions $\mathcal{F}_{NegExp}$ and $\mathcal{F}_{long}$, respectively, are added to take into account the outliers.

The fractions of these contributions and their parameters were determined from the data sample. The background PDF is expressed in the following form:

$$\begin{aligned}
P_{bkg}(x^M, \sigma_{x^M}, \mathcal{D}) &= \left(\mathcal{F}_{peak_bkg} G(x^M, \sigma_{peak_bkg}) + (1 - \mathcal{F}_{peak_bkg}) \cdot P^{res}_{bkg}(x^M, \sigma_{x^M})\right), \quad (28)\\
P^{res}_{bkg}(x^M, \sigma_{x^M}, \mathcal{D}) &= \frac{Eff(x^M)}{N} \int_0^\infty dx \left(\mathcal{F}_0 G(x - x^M, s_{bkg}\sigma_{x^M})\delta(x) + (1 - \mathcal{F}_0) G(x - x^M, \sigma_{x^M}) \cdot p^{long}_{bkg}\right),\\
p^{long,osc/nos}_{bkg}(x, \mathcal{D}) &= e^{\left(-\frac{x}{c\tau_{bkg}}\right)} \left((1 - \mathcal{F}_{tsens}) + \mathcal{F}_{tsens} \left((1 \pm \mathcal{D})(1 - \mathcal{F}_{osc}) + (1 \pm \mathcal{D} \cos(\Delta m_d \cdot x/c)) \cdot \mathcal{F}_{osc}\right)\right),
\end{aligned}$$

where fit parameters were $\mathcal{F}_{peak\_bkg}$, σ_{peak_bkg}, $\mathcal{F}_0$, $\mathcal{F}_{tsens}$, $\mathcal{F}_{osc}$ and $c\tau_{bkg}$. As an efficiency $Eff(x^M)$, the efficiency for the $B_d \to D^{\pm} \mu \nu$ channel was used.

VII. INPUTS TO THE FIT

We used the following measured parameters for B mesons from the PDG [8] as inputs for the fitting procedure: $c\tau_{B^+} = 501$ μm, $c\tau_{B_d} = 460$ μm, and $\Delta m_d = 0.502$ ps^{-1}.

The latest PDG values were also used to determine the branching fractions of decays contributing to the D_s^- sample. We used the event generator EvtGen [16] since this code was developed specifically for the simulation of B decays. For those branching fractions not given in the PDG, we used the values provided by EvtGen, which are motivated by theoretical considerations. Taking into account the corresponding branching fractions and reconstruction efficiencies, we determined the following contributions to our signal region from the various processes in the $\mu\phi\pi$ mode for the RunIIa dataset:

- $B_s^0 \to l^+\nu D_s^-$: $(21.7 \pm 1.2)\%$;
- $B_s^0 \to l^+\nu D_s^{-*} \to l^+\nu D_s^- X$: $(60.7 \pm 3.2)\%$;
- $B_s^0 \to l^+\nu D_{s0}^{*-} \to l^+\nu D_s^- X$: $(1.4 \pm 0.5)\%$;
- $B_s^0 \to l^+\nu D_{s1}^{'-} \to l^+\nu D_s^- X$: $(3.1 \pm 0.5)\%$;
- $B_s^0 \to \tau^+\nu D_s^- \to l^+\nu D_s^- X$: $(1.3 \pm 0.5)\%$;
- $B_s^0 \to D_s^+ D_s^- X; D_s^- \to l\nu X$: $(2.9^{+1.1}_{-2.1})\%$;
- $B_s^0 \to D D_s^- X; D \to l\nu X$: $(0.9 \pm 0.5)\%$;
- $B^+ \to D D_s^- X; D \to l\nu X$: $(4.1 \pm 1.3)\%$;
- $B^0 \to D D_s^- X; D \to l\nu X$: $(4.0 \pm 1.4)\%$;

The numbers for RunIIb and for the other semileptonic modes are similar.

In the above numbers, the reconstruction efficiency does not include any lifetime cuts. We determined the efficiency of the lifetime selections for the sample as a function of VPDL; Fig. 6 shows this function for the decay $B_s \to e^+\nu D_s^- X$.

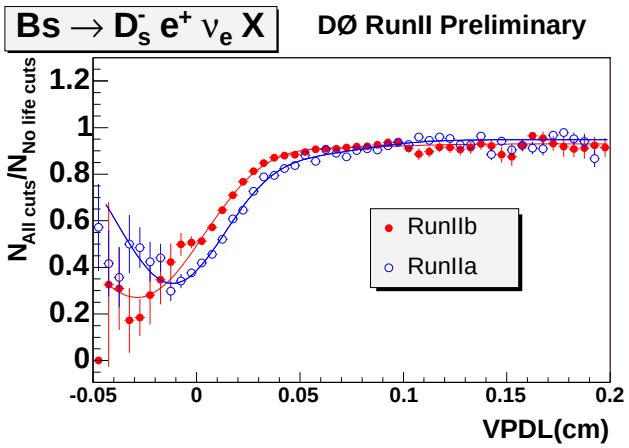

FIG. 6: Efficiency of the lifetime-dependent cuts as a function of VPDL(cm) for $B_s^0 \to e\nu D_s^- X$ from Run IIa and RunIIb MC. RunIIb MC includes simulation of the Layer 0.

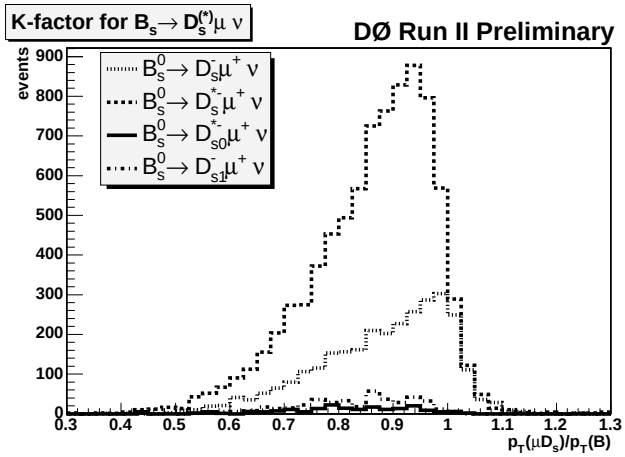

FIG. 7: K factor distributions for $B_s^0 \to \mu^+\nu D_s^-$; $B_s^0 \to \mu^+\nu D_s^{-*} \to \mu^+\nu D_s^-$; $B_s^0 \to \mu^+\nu D_{s0}^{*-} \to \mu^+\nu D_s^-$; $B_s^0 \to \mu^+\nu D_{s1}^{'-} \to \mu^+\nu D_s^-$ processes.

In determining the K factor, MC generator-level information was used for the computation of the transverse momentum, p_T. Following the definition used in (9), the K factors for all considered decays were calculated. Fig. 7 shows the distributions of the K factors for the semi-muonic decays of the B_s meson. As expected, the K factors for D_s^{-*}, D_{s0}^{*-} and $D_{s1}^{'-}$ have lower mean values because more decay products are lost. The K factor for all other B_s^0 decay modes were determined in the same way. Since the K factors in (9) are defined as the ratio of transverse momenta, they can exceed unity.

	RunIIa			RunIIb		
Parameter	$\mu\phi\pi$	$e\phi\pi$	$\mu K^{*0}K^-$	$\mu\phi\pi$	$e\phi\pi$	$\mu K^{*0}K^-$
$\mathcal{F}_0$	0.113 ± 0.004	0.351 ± 0.020	0.08 ± 0.01	0.170 ± 0.002	0.413 ± 0.025	0.00000 ± 0.00005
s_{bkg}	2.11 ± 0.02	1.986 ± 0.003	1.924 ± 0.005	2.08 ± 0.01	2.206 ± 0.005	2.215 ± 0.005
$\sigma_{peak\_bkg}(\mu\text{m})$	127.6 ± 2.4	110 ± 10	0.0 ± 0.0	8.8 ± 0.9	90 ± 20	68 ± 5
$\mathcal{F}_{peak\_bkg}$	0.099 ± 0.004	0.097 ± 0.022	0.0 ± 0.0	0.007 ± 0.002	0.087 ± 0.029	0.030 ± 0.007
$\mathcal{F}_{tsens}$	0.55 ± 0.07	0.58 ± 0.07	0.52 ± 0.08	0.39 ± 0.08	0.62 ± 0.12	0.50 ± 0.25
$\mathcal{F}_{osc}$	0.50 ± 0.08	0.51 ± 0.08	1.00 ± 0.06	0.23 ± 0.17	0.38 ± 0.15	1.00 ± 0.01
$c\tau_{bkg}(\mu\text{m})$	587.8 ± 2.8	690 ± 13	732 ± 3	570.0 ± 2.6	595 ± 23	261 ± 12
$c\tau_{B_s}(\mu\text{m})$	422.2 ± 3.7	444 ± 29	397 ± 26	451.1 ± 4.6	430 ± 59	431 ± 15
$\mathcal{F}_{peak}$	0.036 ± 0.003	0.11 ± 0.03	$0.023(fixed)$	0.043 ± 0.004	0.22 ± 0.05	$0.023(fixed)$
$c\tau_{long}(\mu\text{m})$			340 ± 23			661 ± 15
$\mathcal{F}_{long}$			0.47 ± 0.03			0.409 ± 0.029
$c\tau_{NegExp}(\mu\text{m})$			43.7 ± 9.5			40.4 ± 5.0
$\mathcal{F}_{NegExp}$			0.031 ± 0.008			0.013 ± 0.004

TABLE III: Lifetime fit parameters

The VPDL uncertainty was estimated by the vertex fitting procedure. A resolution scale factor is introduced to take into account a possible bias. It was determined using a $J/\psi \to \mu\mu$ sample. The negative tail of the pull distribution of the J/ψ vertex position with respect to that of the primary vertex should be a Gaussian with a sigma of unity if uncertainties assigned to the vertex coordinates are correct. For this study we excluded muons from J/ψ decays from the primary vertex. The resulting RunIIa and RunIIb pull distributions were fitted separately using a double Gaussian.

For the RunIIa data in the hadronic and $\mu\phi\pi$ modes, an event-by-event scale factor was used to scale the estimated impact parameter uncertainty from the tracking algorithm to the actual impact parameter uncertainty, as the tracking usually underestimates this uncertainty. Detailed information on the method used to obtain the event-by-event scale factor can be found in Reference [17].

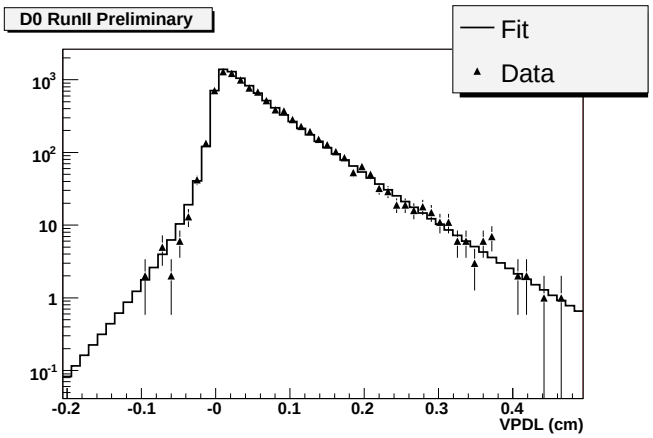

FIG. 8: Distribution of the VPDL in the signal peak region $1.92 < M(D_s) < 2.02$ GeV/c^2 for all tagged candidates in $B_s^0 \to \mu^+ D_s^- X$, $D_s^- \to K^{*0}K^-$ for RunIIb data. The points represent the experimental data, the histogram the fitting function.

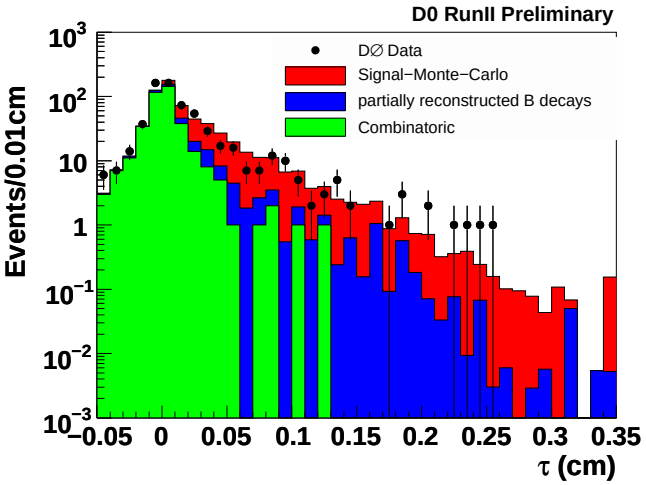

FIG. 9: Distribution of the VPDL for all tagged candidates in $B_d \to \pi^+ D^{*-} X$, $D^{*-} \to K^-\pi^+\pi^-$ for RunIIb data. The points represent the experimental data, the histogram the fitting function.

VIII. RESULTS OF THE LIFETIME FIT

The total tagged data sample was used to determine the parameters: $\mathcal{F}_{peak\_bkg}$, σ_{peak_bkg}, $\mathcal{F}_0$, s_{bkg}, $c\tau_{bkg}$, $\mathcal{F}_{peak}$, $\mathcal{F}_{tsens}$, $\mathcal{F}_{osc}$ and B_s-lifetime $c\tau_{B_s}$ for the semileptonic modes, which are summarized for each channel in Table III.

Figure 8 shows distribution of the VPDL with optimal fit parameters in the fitting function for $\mu K^{*0}K$ mode. Only

VPDL PDFs were used for this plot. The differences between the data points and prediction were addressed in the systematic uncertainties.

A cross check of the lifetime measurement technique for the hadronic decay of B_s^0mesons was performed with sample of B_d^0mesons in a similar decay mode. This analysis has been performed on RunIIa data only, which corresponds to an integrated luminosity of $\int \mathcal{L}\, dt = 1.3$ fb^{-1}. The advantage of this mode is the higher statistics production of the B_d^0 particles. The selection of D^*mesons to reconstruct B_d^0 decays is similar to the selection performed for the B_s^0 decays. From the data a value of $\tau_{B_d} = 1.48^{+0.12}_{-0.10}$ ps has been extracted, which is in good agreement with the world average $\tau_{B_d} = 1.530 \pm 0.009$ ps [8].

IX. RESULTS

Figures 10-13 show the dependence of the parameter $\mathcal{A}$ from (27) and its uncertainties on the Δm_s for different modes for RunIIa and RunIIb combined using a weighted average of the values and uncertainties. We combine the results for different modes for both RunIIa and RunIIb periods into a single amplitude by doing a weighted average of the values and uncertainties. In order to take into account correlations between systematic uncertainties in the various run periods and the different modes, the amplitudes are combined using the "COMBOS" program [18]. The combined amplitude scan for the combined modes (Semileptonic+Hadronic) with statistical and systematic uncertainties is shown in Fig. 14. The combined result, expressed as a likelihood scan, is shown in Fig. 16. We plot

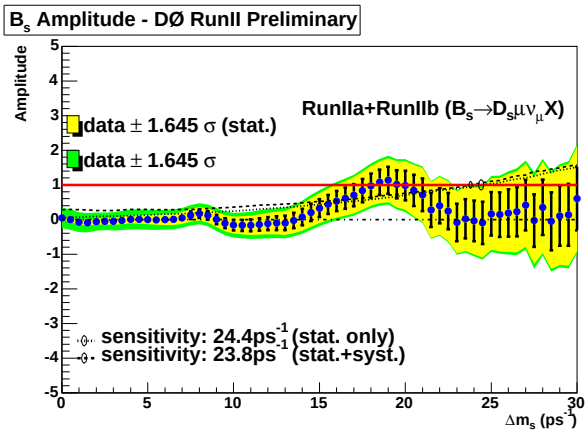

FIG. 10: B_s^0 oscillation amplitude for the $\mu\phi\pi$ mode.

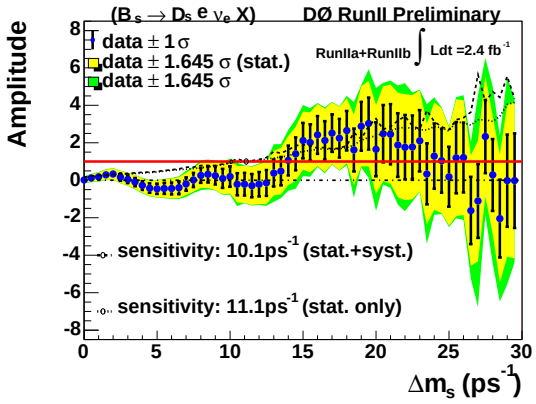

FIG. 11: B_s^0 oscillation amplitude for $e\phi\pi$ mode.

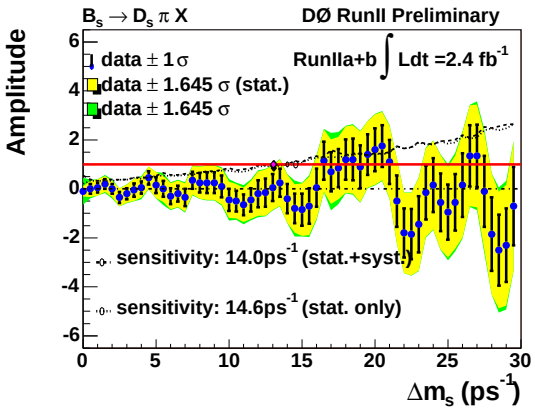

FIG. 12: B_s^0 oscillation amplitude for the $\pi\phi\pi$ mode.

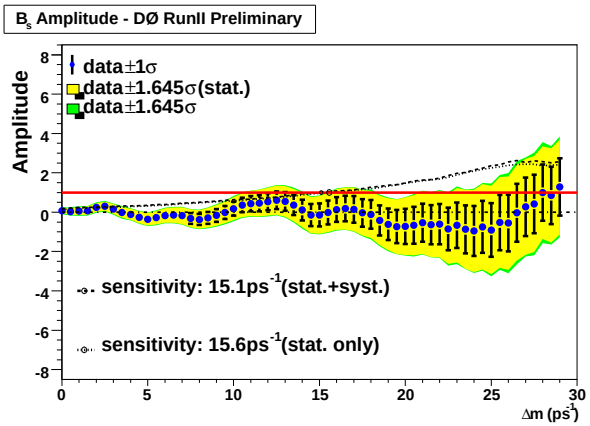

FIG. 13: B_s^0 oscillation amplitude for $\mu K^{*0} K$ mode.

the difference $\Delta logL(\Delta m_s) = logL_{\Delta m_s}(\mathcal{A} = 1) - logL_\infty = 0.5 \times ((\frac{1-\bar{\mathcal{A}}}{\sigma_{\mathcal{A}}})^2 + (\frac{\bar{\mathcal{A}}}{\sigma_{\mathcal{A}}})^2)$, where $\bar{\mathcal{A}}$ is the measured value of the amplitude. We fit the points to a parabolic function and we measure $\Delta m_s = 18.56 \pm 0.87$. The statistical significance of the observed minimum in the likelihood scan is 3.1σ.

The combined semileptonic mode alone yields $\Delta m_s = 18.27 \pm 0.99$ with a statistical significance of 2.7σ. The combined semileptonic result can be seen in Figs. 17 and 19.

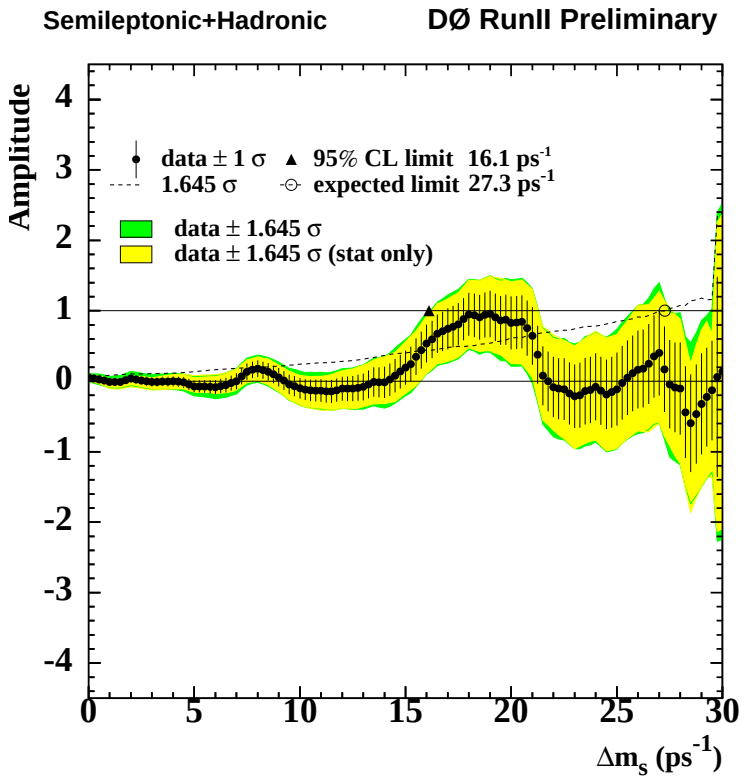

FIG. 14: Combined (Semileptonic+Hadronic) amplitude as a function of Δm_s with statistical and systematic uncertainties.

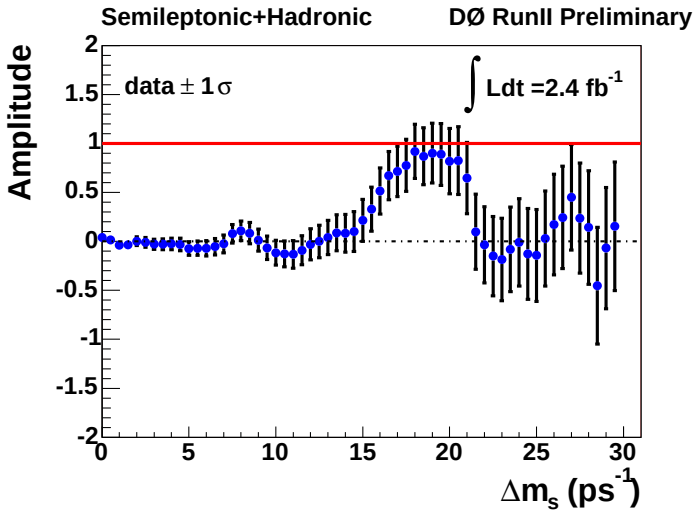

FIG. 15: Combined (Semileptonic+Hadronic) amplitude as a function of Δm_s with statistical errors only and only showing 1σ errors.

X. SYSTEMATIC UNCERTAINTIES AND CROSS CHECKS

The following sources of the systematic uncertainties were considered for the semileptonic modes:

- Variation in sample composition due to changing $\mathrm{Br}(D_s D_s) = 4.7\%$ (Default: 22.5%)
- Variation in sample composition due to changing $\mathrm{Br}(D_s \mu X) = 6.7\%$ (Default:7.9%)

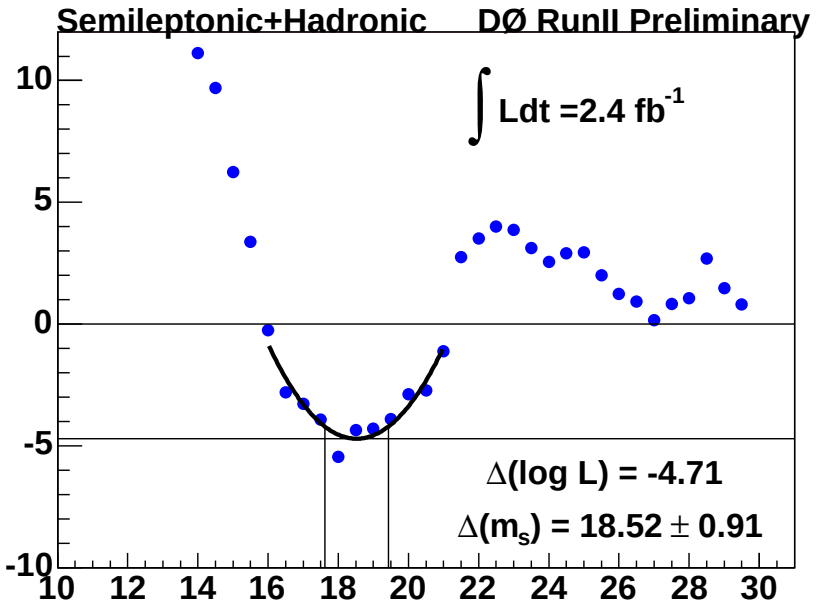

FIG. 16: Dependence of $\Delta(log\mathcal{L})$ on Δm_s for semileptonic and hadronic modes combined

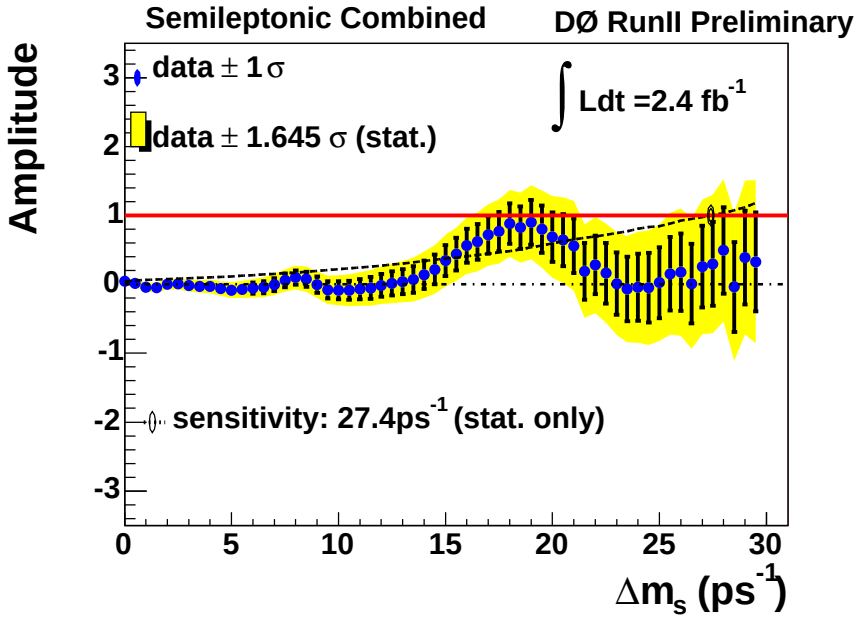

FIG. 17: Combined amplitude as a function of Δm_s for semileptonic modes with statistical uncertainties alone.

- K-factor variation 2%, K-factor distribution smoothed.
- Variation of the background and signal fractions and other fit parameters obtained from the lifetime fit, within fit errors, as listed in table III.
- statistical fluctuation of N_{D_s} and reflections.
- Signal resolution (s_{sig} (Eqn. 24)), Background resolution (s_{bkg} (Eqn. 28))

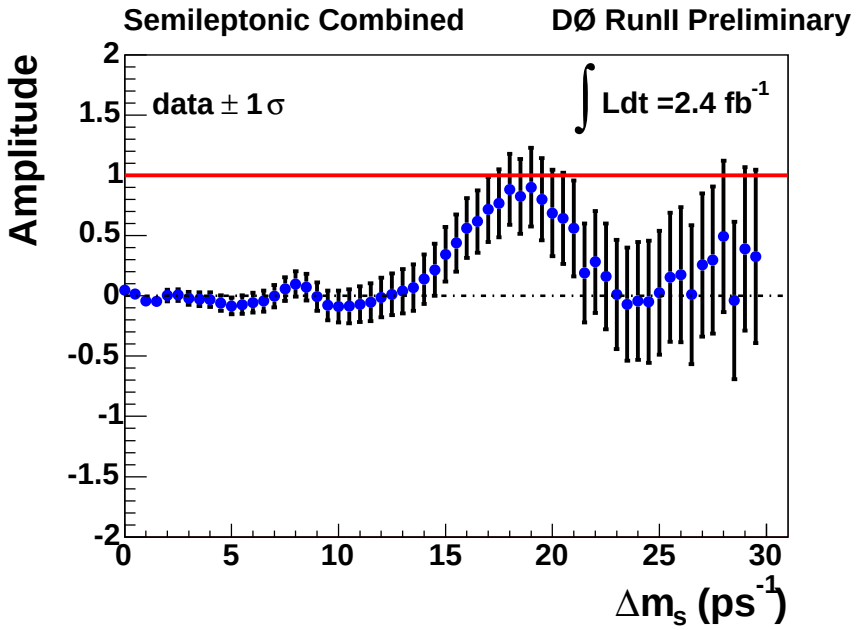

FIG. 18: Combined amplitude as a function of Δm_s for semileptonic modes with statistical uncertainties alone showing 1σ errors.

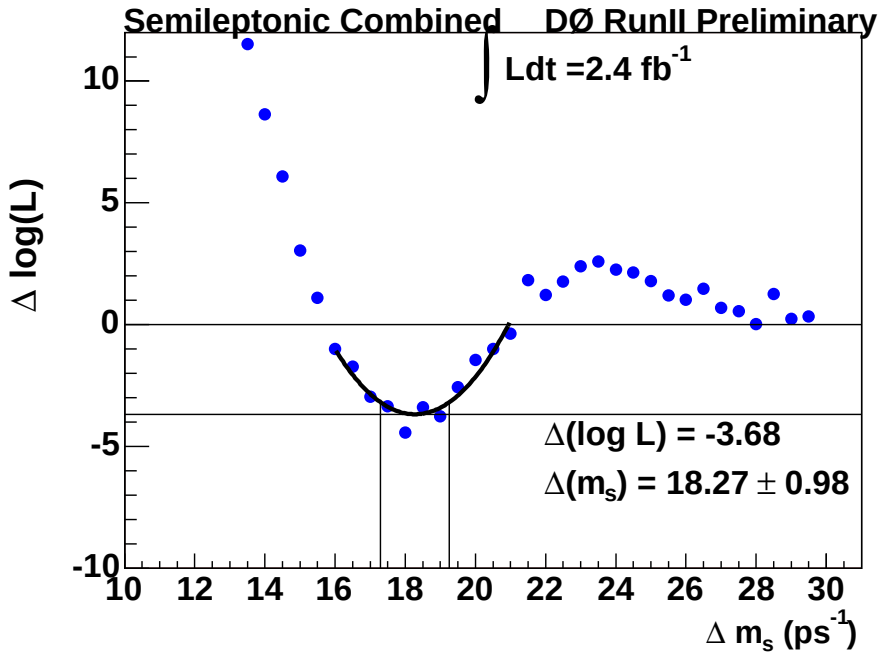

FIG. 19: Dependence of $\Delta(log\mathcal{L})$ on Δm_s for semileptonic modes only.

- variation of dilution calibration within error bands
- non-zero $\frac{\Delta\Gamma}{\Gamma}$
- B_s lifetime fixed to PDG value instead of obtaining it from fit.
- Flat Efficiency as a function of lifetime vs default efficiency parametrization as a function of lifetime (Fig. 6).

For each Δm_s step, the deviations of $\Delta\mathcal{A}$ and $\Delta\sigma$ are obtained and the resulting systematic uncertainties were obtained using the formula ([15])

$$\sigma_{\mathcal{A}}^{sys} = \Delta\mathcal{A} + (1-\mathcal{A})\frac{\Delta\sigma_{\mathcal{A}}}{\sigma_{\mathcal{A}}}, \tag{29}$$

and were summed in quadrature. The effect of the systematic uncertainties is represented by the green (dark grey) region in Figs. 10- 13. and in the combined scan, Fig. 14.

The decays $B_d \to Xl D^{\pm}(\to \phi\pi)$ (the left-side peak in Fig. 2) allow for a cross check of the entire fitting procedure using the same data sample as for the signal $B_s \to Xl D_s(\to \phi\pi)$ events. Figure 20 shows the dependence of the parameter $\mathcal{A}$ and its uncertainty on Δm_d. The peak in the amplitude scan at $\Delta m_d \approx 0.5$ ps^{-1} reveals the oscillations in the B_d—$\bar{B}_d$ system for the $l \equiv \mu$ mode. The peak amplitude is in agreement with unity, which confirms that the dilution calibration is correct.

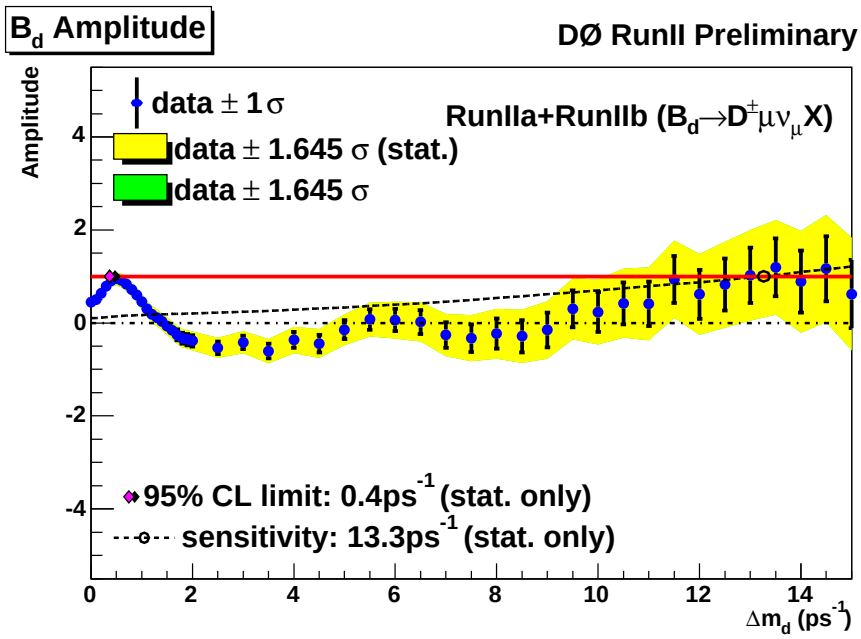

FIG. 20: B_d oscillation amplitude with statistical uncertainty only for the $\mu\phi\pi$ mode.

XI. CONCLUSIONS

Using fully reconstructed hadronic and partially reconstructed hadronic and semileptonic decay modes of the B_s meson a combined opposite- and same-side initial-state flavor-tagging algorithm and an unbinned fit, we measured the $B_s^0 - \bar{B}_s^0$ oscillation frequency to be $\Delta m_s = 18.56 \pm 0.87$ ps^{-1}. The statistical significance of the measurement exceeds 3σ.

Acknowledgments

We thank the staffs at Fermilab and collaborating institutions, and acknowledge support from the DOE and NSF (USA); CEA and CNRS/IN2P3 (France); FASI, Rosatom and RFBR (Russia); CAPES, CNPq, FAPERJ, FAPESP and FUNDUNESP (Brazil); DAE and DST (India); Colciencias (Colombia); CONACyT (Mexico); KRF (Korea); CONICET and UBACyT (Argentina); FOM (The Netherlands); PPARC (United Kingdom); MSMT (Czech Republic); CRC Program, CFI, NSERC and WestGrid Project (Canada); BMBF and DFG (Germany); SFI (Ireland);

Research Corporation, Alexander von Humboldt Foundation, and the Marie Curie Program.

---

[1] A. Abulencia, *et al.*, Phys. Rev. Lett. **97** (2006) 242003.
[2] V. Abazov, *et al.*, Phys. Rev. Lett. **97** (2006) 021802.
[3] V. Abazov *et al.* [DØ Collaboration] *The Upgraded DØ Detector*, submitted to Nucl. Instrum. Methods Phys. Res. A., arXiv:hep-physics/0507191, Fermilab-Pub-05/341-E.
[4] V. M. Abazov *et al.*, Nucl. Instrum. Meth. A **552**, 372 (2005).
[5] Charge conjugate states are assumed throughout this paper.
[6] S. Catani, Yu.L. Dokshitzer, M. Olsson, G. Turnock, B.R. Webber, Phys.Lett. **B269** (1991) 432.
[7] T. Sjöstrand *et al.*, hep-ph/0108264.
[8] Particle Data Group, Review of Particle Physics, J. Phys. **G 33**, 1 (2006).
[9] DELPHI Collab., *b-tagging in DELPHI at LEP*, Eur. Phys. J. **C32** (2004), 185-208.
[10] DØ Collaboration, B_s Mixing studies with $B_s^0 \to D_s^- \mu^+ X$ ($D_s^- \to K^{*0} K^-$) Decay using Unbinned Fit, DØ Conference Note: 5172
[11] V. Abazov *et al.* [DØ Collaboration], "Measurement of B_d mixing using opposite-side flavor tagging", Phys. Rev. **D74**,(2006) 112002.
[12] DØ Collaboration, "Combination of Same-Side Taggers for B_s Mixing Study", DØ Conference Note: 5210.
[13] F. James, *MINUIT - Function Minimization and Error Analysis*, CERN Program Library Long Writeup D506, 1998.
[14] DØ Collaboration, Phys. Rev. Lett. 94, 182001 (2005).
[15] H.G. Moser, A. Roussarie, Nucl.Instrum.Meth.A384:491–505, 1997.
[16] D.J. Lange, Nucl.Instrum.Meth.A462:152, 2001; for details see *http://www.slac.stanford.edu/~ lange/EvtGen*.
[17] G. Borissov and C. Mariotti, NIM A 372 (1996) 181.
[18] Heavy Flavor Averaging Group, *http://www.slac.stanford.edu/xorg/hfag/index.html*.